Effect of external magnetic field on the shift of resonant frequency in photoassociation of ultracold Cs atoms*

Pengwei Li(李鹏伟)[1], Yuqing Li(李玉清)[1,2,†], Guosheng Feng(冯国胜)[1], Jizhou Wu(武寄洲)[1,2], Jie Ma(马杰)[1,2], Liantuan Xiao(肖连团)[1,2], and Suotang Jia(贾锁堂)[1,2]

[1] *State Key Laboratory of Quantum Optics and Quantum Optics Devices, Institute of Laser Spectroscopy, College of Physics and Electronics Engineering, Shanxi University, Taiyuan* 030006, *China*
[2] *Collaborative Innovation Center of Extreme Optics, Shanxi University, Taiyuan* 030006, *China*

(Received 27 September 2018; revised manuscript received 22 November 2018; published online 12 December 2018)

We study the influence of external magnetic field on the shift of the resonant frequency in the photoassociation of ultracold Cs atoms, which are captured in a magnetically levitated optical crossed dipole trap. With the increase of the photoassociation laser intensity, the linear variation of the frequency shift is measured by recording the photoassociation spectra of the long-range 0_u^+ state of Cs molecule below the $6S_{1/2}+6P_{1/2}$ dissociation limit at different magnetic fields. The slope of the frequency shift to the intensity of the photoassociation laser exhibits a strong dependence on the external magnetic field. The experimental data is simulated with an analytic theory model, in which a single channel rectangular potential with the tunable well depth is introduced to acquire the influence of the magnetic field on the atomic behavior in the effective range where photoassociation occurs.

Keywords: ultracold molecule, photoassociation, frequency shift

PACS: 37.10.Pq, 37.10.Mn, 33.70.Jg **DOI:** 10.1088/1674-1056/28/1/013702

1. Introduction

The formation and manipulation of ultracold molecules have been attracting a large amount of research interest due to their potential applications.[1] Ultracold molecules as the basic units of chemical matter at ultralow temperatures provide an efficient way to coherently control the chemical reaction at vanishing entropy.[2,3] Their rich internal structure is available to obtain higher accuracy in the precise measurement of fundamental physical constants.[4–8] The strong dipolar interaction of ultracold heteronuclear molecules induced by an external electric field can be used for the quantum simulation of the strongly interacting regime and quantum computation.[9,10] In this context, the photoassociation (PA) of ultracold atoms is a common but vital tool for the formation of ultracold molecules, which has been extensively investigated to facilitate the promising applications of ultracold molecules.[11–16]

In PA spectra, an interesting phenomenon is the shift of the resonant transition frequency from ground atoms to excited molecules, which has to be considered for the efficient formation of ultracold molecules.[17] The shift is mainly attributed to the coupling between the scattering atomic state and excited molecular state. The shift has a strongly linear dependence on the intensity of the PA laser.[18,19] A large number of atomic species have been experimentally studied for exhibiting the frequency shift of PA laser-induced transition.[20–25] In these previous studies, the slope of the shift to PA laser intensity has been illustrated as an efficient way to measure the s-wave scattering length of colliding atoms.[26] It is also closely related to both the optical Feshbach resonance of alkali-metal atoms[27] and the formation of ultracold molecules.[17] However, there are very few studies on the effect of the external field on the slope and the techniques that are likely to alter the slope and manipulate the frequency shift in PA spectra.

Although Feshbach resonance of ^{7}Li atoms has been experimentally confirmed to have a great influence on the shift of the transition frequency in the PA,[28] the result is only qualitatively explained and quantitative investigations are still lacking. In this paper, we present the variation of the shift of the resonant transition frequency in the PA of ultracold Cs atoms with the intensity of the PA laser at different magnetic fields. We develop a square well model with a tunable depth, where the magnetic field can be used to alter the atomic collision during the PA of ultracold atoms. The quantitative analysis agrees with the observed dependence of the slope of the shift on the external magnetic field.

2. Experimental setup

The Cs atoms are collected and prepared in a standard vapor-loaded magneto-optical trap (MOT). Successively compressed MOT and optical molasses are implemented to in-

*Project supported by the National Key Research and Development Program of China (Grant No. 2017YFA0304203), the Chang Jiang Scholars and Innovative Research Team in the University of the Ministry of Education of China (Grant No. IRT13076), the National Natural Science Foundation of China (Grant Nos. 61722507, 61675121, 61705123, and 11434007), the Fund for Shanxi 1331 Project Key Subjects Construction, China, and the Applied Basic Research Project of Shanxi Province, China (Grant No. 201701D221002).

†Corresponding author. E-mail: lyqing.2006@163.com

crease the atomic density and lower the temperature of the atomic sample by increasing the magnetic field gradient, reducing the intensity of the repumping laser, and enlarging the detuning of the trapping laser. Furthermore, the pre-cooled atoms are efficiently loaded into a three-dimensional (3D) optical lattice, which consists of four linearly polarized far-off-resonance laser beams with an optically optimized frequency detuning.[29] The degenerated Raman sideband cooling (DRSC) is then performed by pumping the degenerated adjacent vibrational levels with the different Zeeman sublevels to a dark state with the lowest vibrational number of $v = 0$ at the magnetic field of ~ 200 mG. Through 10 ms of 3D DRSC, the atoms are cooled to the temperature of ~ 1.7 μK and prepared in the $F = 3$, $m_F = 3$ state.

After the 3D DRSC, the 3D optical lattice is adiabatically released with a 1/e time of 100 μs. Meanwhile, a crossed optical dipole trap is used to collect the cooled atoms, where two 1064 nm, high-power of ~ 7 W laser beams are focused on the center of the atomic sample with the 1/e beam radius of ~ 240 μm at the crossing angle of 90°, as shown in Fig. 1. Considering the large gravity of the Cs atom, the magnetic levitation is employed to cancel the gravity during the loading of the crossed dipole trap.[30] The magnetically levitated loading of the optical trap is performed by applying both the magnetic field gradient of 31.13 G/cm and the bias field of 75 G in the vertical direction. The plain evaporation of 500 ms is subsequently implemented for the optically trapped atoms by the three-body loss-dominating thermal equilibrium at a bias field of 75 G, after which the number of atoms trapped in the optical trap is measured as about 2.5×10^5 with the temperature of 3.5 μK.

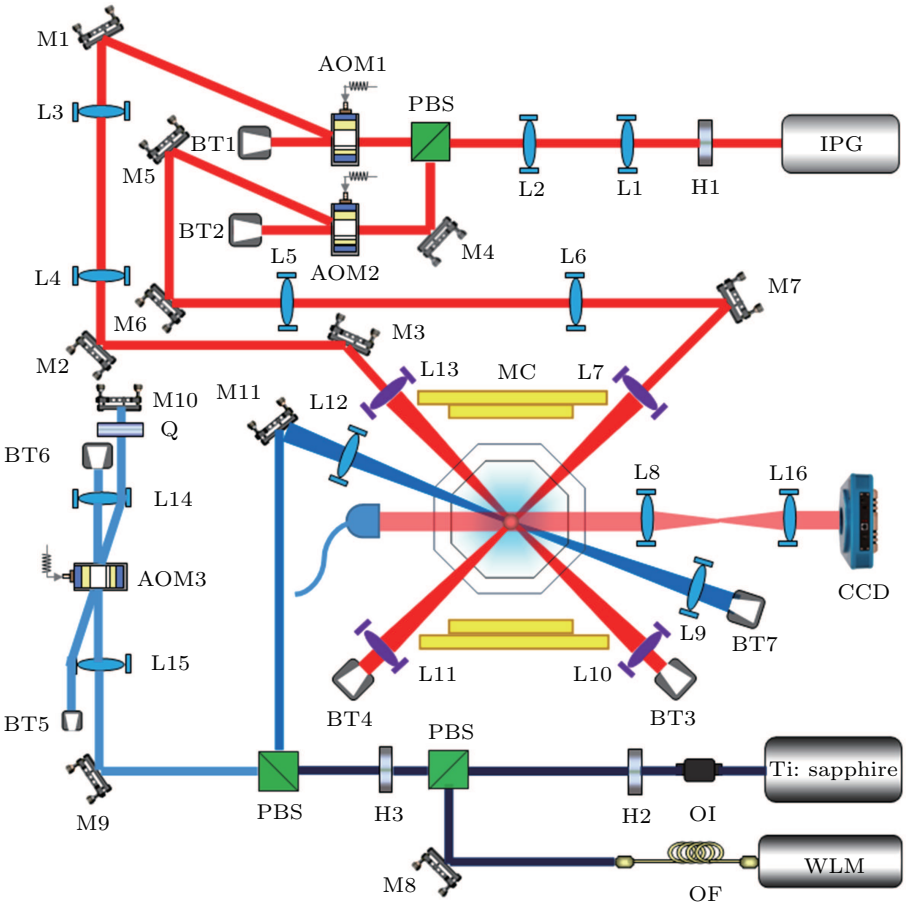

Fig. 1. Experimental setup for the PA of ultracold Cs atoms in a magnetically levitated crossed dipole trap at different magnetic fields. IPG, high power fiber laser; WLM, wavelength meter; OI, optical isolator; OF, optical fiber; AOM, acousto-optic modulator; BT, beam trap; L, lens; H, half-wave plate; Q, quarter-wave plate; M, mirror; PBS, polarization beam splitter; MC, magnetic field coil; CCD, charge-coupled device.

PA is performed by illuminating a narrow linewidth Ti:sapphire laser with the widely tunable output frequency on the atomic sample in the optical trap for 100 ms. The PA laser is focused on the center of the atomic cloud with a beam waist of 150 μm. When the frequency of the PA laser is resonantly tuned to the transition frequency from the scattering atom state to the excited molecular state, the number of remaining atoms in the optical trap reduces because the formed weakly excited molecules spontaneously decay either into pairs of hot atoms that escape the trap or into the ground state molecules. Therefore PA spectroscopy can be obtained by recording the number of atoms in the dipole trap as a function of the PA laser

frequency, which is monitored by a high precision wavemeter (HighFinese WSU). The frequency of the PA laser is tuned to ~ 11155.059 cm^{-1} near the resonant transition from the scattering state $F = 3$, $m_F = 3$ of Cs atoms to the rovibrational level of $v_D - v = 190$, $J = 0$ of the excited Cs_2 0_u^+ state below the $6S_{1/2}+6P_{1/2}$ dissociation limit.[31] The number of atoms in the trap after PA is experimentally detected with the variable detuning of the PA laser in a large number of experimental cycles. A typical PA spectrum is shown in Fig. 2 with the intensity of PA laser $I_{PA} = 120$ W/cm^2 at the bias field of $B = 75$ G.

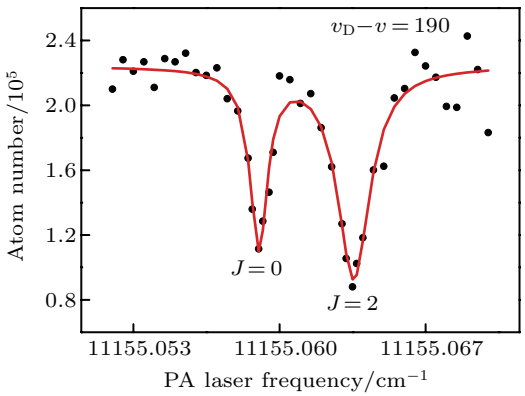

Fig. 2. PA spectrum of the $v_D - v = 190$ molecular vibrational level for $J = 0$ and $J = 2$ in Cs_2 long-range 0_u^+ state below the $6S_{1/2}+6P_{1/2}$ dissociation limit.

3. Experimental results and analysis

The shift of the resonant transition frequency in the PA of ultracold colliding atoms is induced by the change of the PA laser intensity I_{PA}. As the intensity of the PA laser varies in each experimental cycle, the position at which the number of optically trapped atoms exhibits the maximum loss shifts in the PA spectrum. Figure 3 shows the variations of the shifts of the PA transition frequencies with the increasing I_{PA} for three different magnetic fields of $B = 35$ G, 60 G, and 85 G. For each magnetic field, the shift shows a linear dependence on I_{PA} as predicted in Ref. [18]. Interestingly, the application of external magnetic field has an effect on the variation of the frequency shift with I_{PA}, as shown in Fig. 3. By linearly fitting the variations of the shifts with I_{PA} at three different magnetic fields, the slopes of the shifts are derived as 1.363 MHz/(W/cm^2), 1.881 MHz/(W/cm^2), and 2.092 MHz/(W/cm^2) corresponding to the magnetic fields of $B = 35$ G, 60 G, and 85 G, respectively.

According to the simple and approximate expression of the frequency shift in Refs. [27] and [32], the magnitude of the shift of the transition frequency in PA is given as $\beta\Omega^2/\delta\varepsilon_v$, where $\Omega = (\Gamma_a^2/2)I/I_{sat}$, Γ_a is the linewidth of Cs atom, I_{sat} is the atomic saturation intensity, $\delta\varepsilon_v$ is the energy difference between the vibrational levels v and $v+1$, and $\beta = \int |\langle\psi_{v,J}|\phi_k\rangle| \mathrm{d}r$ is a numeric factor that characterizes the overlap integral between the ground atomic and excited molecular wavefunctions. The frequency shifts in Fig. 3 show the linear dependence on the intensity of the PA laser at three different magnetic fields, which agrees with the previous theoretical expression that the shift is proportional to the intensity of the PA laser.

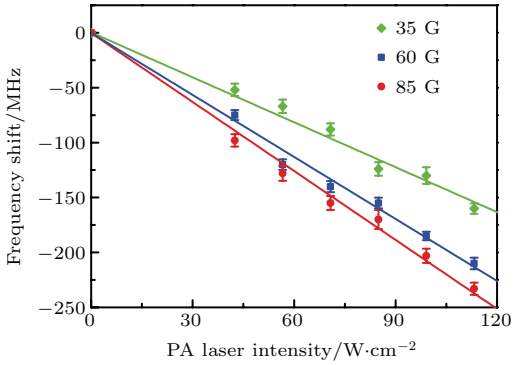

Fig. 3. The frequency shift as a function of PA laser intensity for the rovibrational level of $v_D - v = 190$, $J = 0$ of Cs_2 0_u^+ long-range state at three different magnetic fields. The color curves are the linear fittings for the variations of the frequency shifts on the intensity of PA laser at the external magnetic fields of 35 G (green diamonds), 60 G (blue squares), and 85 G (red circles).

For the variation of the slope of the frequency shift in PA with the magnetic field, there is only a qualitative explanation for the previously experimental observations by considering the direct effect of the external magnetic fields on the coupling strength between the atomic and excited molecular states.[28] In the low temperature limit, the magnetic field alters the atomic s-wave scattering length and then leads to the variation of the scattering phase shift, which is a significant parameter in the atomic wavefunction. Nevertheless, the atomic scattering wavefunction in a long range is insufficient to capture the behavior of the colliding atoms in the effective range in which PA occurs.

An analytically theoretical model in Ref. [33] was used to calculate the atomic scattering length near a Feshbach resonance, and this model was used to explain the enhanced PA by magnetic field.[34] Here, a single channel square-well potential with a tunable depth is considered to generate a versatile wavefunction of Cs atoms in the effective PA range in Fig. 4(a) and then applied to the obtained variation of the slope of the frequency shift with the magnetic field in Fig. 4(b). The single channel square-well potential model is introduced by dividing interatomic separation r into two regions: the inner region $r < R_0$ where the exchange interaction is much larger than the hyperfine splitting, and the outer region $r > R_0$ where the hyperfine interaction dominates,

$$\phi_k(r) = \phi_{k,r>R_0}(r) + \phi_{k,r<R_0}(r). \quad (1)$$

The radius of the model square-well potential is chosen to be the mean scattering length $R_0 = \bar{a} = 4\pi\Gamma(1/4)^{-2}R_{vdW}$,[35] where $R_{vdW} = (2m_rC_6/\hbar)^{1/4}/2$ is the van der Waals radius, m_r is the reduced mass, and C_6 is the van der Waals coefficient at

R^{-6} in the realistic long-range potential. The mean scattering length of $95.7a_0$ securely covers the range of the upper bound state wavefunction of the excited Cs molecule. The atomic scattering wavefunction in the range of $r > R_0$, containing the incident plane wave and a scattered wave, approaches

$$\phi_{k,r>R_0}(r) = \sqrt{\frac{k}{\pi E}}\sin(kr+\eta), \tag{2}$$

where $E = h^2k^2/2m_r$ is the colliding energy of atoms and η is the scattering phase shift. The s-wave collision of ultracold atoms gives a precise statement of η as[36]

$$k\cos\eta = -1/a + \frac{1}{2}r_0k^2, \tag{3}$$

where a is the scattering length and r_0 is defined as the effective range. In the region of $r < R_0$, the atomic wavefunction is given by

$$\phi_{k,r<R_0}(r) = A\sin(k_1 r), \tag{4}$$

where A is the amplitude of the atomic wavefunction, the wave vector $k_1 = \sqrt{m(E+V_p)}/h$, and V_p is the square-well potential.

For ^{133} Cs atoms in the hyperfine state $F = 3$, $m_F = 3$, the s-wave Feshbach resonance of $B = -11.74$ G leads to the smooth variation of the scattering length a in the low-field region from 0 to 150 G and the dependence of the scattering length on B can be well approximated as[37,38]

$$a(B)/a_0 = (1722 + 1.52B/G) \times \left(1 - \frac{28.72}{B/G + 11.74}\right), \tag{5}$$

except for a few narrow Feshbach resonances. Thus, we can alter the atomic wavefunction $\phi_{k,r>R_0}(r)$ by changing the magnetic field, which determines the atomic scattering length and then affects the scattering phase shift contained in the expression of $\phi_{k,r>R_0}(r)$.

Compared to the radius of the square-well potential R_0, the small effective range of the excited molecule state wavefunction $\psi_{v,J}(r)$ determines that only the atomic wavefunction $\phi_{k,r<R_0}(r)$ in the region of $r < R_0$ dedicates to the effective overlap between the atomic and molecular wavefunctions. To explain the observed variation of the slope with the magnetic field, we construct the tunable depth of the square-well potential in Fig. 4(a) to present a variable vector k_1 of the wavefunction $\phi_{k,r<R_0}(r)$, which conforms the requirement of the wavefunction itself and its first derivative to be continuous at the switching point R_0. As a result, the magnetic field can be used to alter the wavefunction of colliding atoms in the effective region where PA occurs and then affects the overlap between the atomic and molecular wavefunctions in the calculation of the slope of the PA frequency shift. According to the Franck–Condon principle, PA predominately occurs at the classical outer turning point R_c of the excited rovibrational energy state, and so $\beta \propto |\phi_{k,r<R_0}(R_c)|$. For the molecular rovibrational level $v_D - v = 190$, $J = 0$ of the excited Cs_2 0_u^+ state below the $6S_{1/2}+6P_{1/2}$ dissociation limit, the classical outer turning point is $R_c \approx 49a_0$. By analytically calculating β with an appropriate ratio, the theoretically obtained result is shown in Fig. 4(b), and the theory shows good agreement with the measurement.

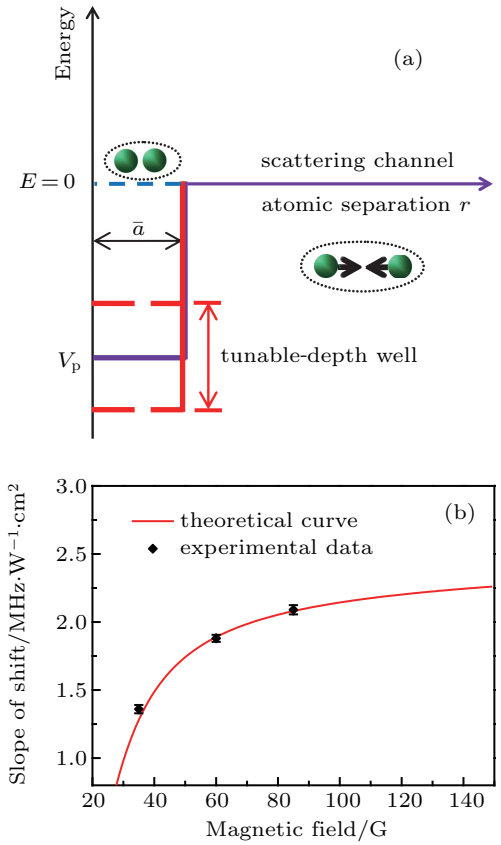

Fig. 4. (a) Illustration of single channel square-well potential with the tunable depth. The horizontal line in the outer region represents the potential energy $U = 0$. An external magnetic field can alter the scattering length of colliding atoms in the outer region and then induces the variation of the atomic wavefunction, whose continuity at the boundary point R_0 requires the tunable-depth square well potential indicated by the dashed lines. As a result, the magnetic field can change the density of the atomic pairs in the short internuclear distance where PA occurs. (b) The slope of the frequency shift derived from Fig. 3 as a function of magnetic field. The black diamond is experimental data and the red solid line is the theoretical result.

4. Conclusion

We have presented the linear dependence of the frequency shift on the intensity of the PA laser at three different magnetic fields. The derived slope of the shift is strongly dependent on the magnetic field, which has potential applications on the formation of cold molecules, precision measurement, and coherent manipulation of atoms and molecules. The observed variation of the slope with magnetic field is reproduced with a reasonable quality by using the model of a single-channel square-well potential with the tunable depth. Through this model, we can relate the magnetic field to the atomic wavefunction in

the effective PA region. In the previous experiments, the influence of magnetic field on the shift in PA was explained by directly considering that the magnetic field controlled scattering length alters the atomic scattering wavefunction outside of the effective PA range. In contrast, our result shows the clear physical mechanism for the effect of external magnetic field on the slope of the frequency shift in PA.

References

[1] Carr L D, DeMille D, Krems R V and Ye J 2009 *New J. Phys.* **11** 055049
[2] Krems R, Friedrich B and Stwalley W C 2009 *CRC Press* **753** 279
[3] Krems R V 2005 *Int. Rev. Phys. Chem.* **24** 99
[4] Zelevinsky T, Kotochigova S and Ye J 2008 *Phys. Rev. Lett.* **100** 043201
[5] DeMille D, Sainis S, Saga J, Bergeman T, Kotochigova S and Tiesinga E 2008 *Phys. Rev. Lett.* **100** 043202
[6] Beloy K, Borschevsky A, Flambaum V V and Schwerdtfeger P 2011 *Phys. Rev. A* **84** 042117
[7] Sainis S, Saga J, Tiesinga E, Kotochigova S, Bergeman T and DeMille D 2012 *Phys. Rev. A* **86** 022513
[8] Ma J, Chen P, Liu W L, Feng G S, Li Y Q, Wu J Z, Xiao L T and Jia S T 2013 *Acta Phys. Sin.* **62** 223301 (in Chinese)
[9] Micheli A, Brennen G K and Zoller P 2006 *Nat. Phys.* **2** 341
[10] DeMille D 2002 *Phys. Rev. Lett.* **88** 067901
[11] Fioretti A, Comparat D, Crubellier A, Dulieu O, Masnou-Seeuws F and Pillet P 1998 *Phys. Rev. Lett.* **80** 4402
[12] Yan B, Moses S A, Gadway B, Covey J P, Hazzard K R A, Rey A M, Jin D S and Ye J 2013 *Nature* **501** 521
[13] Molony P K, Gregory P D, Ji Z, Lu B, Köpinger M P, Sueur C R L, Blackley C L, Hutson J M and Cornish S L 2014 *Phys. Rev. Lett.* **113** 255301
[14] Park J W, Will S A and Zwierlein M W 2015 *Phys. Rev. Lett.* **114** 205302
[15] Zhang W, Xie T, Huang Y, Wang G R and Cong S L 2013 *Chin. Phys. B* **22** 013301
[16] Wang Y, Yue D G, Zhou X C, Guo Y H and Meng Q T 2017 *Chin. Phys. B* **26** 043202
[17] Jones K M, Tiesinga E, Lett P D and Julienne P S 2006 *Rev. Mod. Phys.* **78** 483
[18] Bohn J L and Julienne P S 1999 *Phys. Rev. A* **60** 414
[19] Liu W, Wang X, Wu J, Su X, Wang S, Sovkov V B, Ma J, Xiao L and Jia S 2017 *Phys. Rev. A* **96** 022504
[20] Portier M, Moal S, Kim J, Leduc M, Cohen-Tannoudji C and Delieu O 2006 *J. Phys. B* **39** S881
[21] Prodan I D, Pichler M, Junker M, Hulet R G and Bohn J L 2003 *Phys. Rev. Lett.* **91** 080402
[22] McKenzie C, Denschlag J H, Häffner H, Browaeys A, Araujo L E E, Fatemi F K, Jones K M, Simsarian J E, Cho D, Somoni A, Tiesinga E, Julienne P S, Helmerson K, Lett P D, Rolston S L and Phillips W D 2002 *Phys. Rev. Lett.* **88** 120403
[23] Simoni A, Julienne P S, Tiesinga E and Williams C J 2002 *Phys. Rev. A* **66** 063406
[24] Wu J Z, Ji Z H, Zhang Y C, Wang L R, Zhao Y T, Ma J, Xiao L T and Jia S T 2011 *Opt. Lett.* **36** 2038
[25] Zhang Y C, Ma J, Li Y Q, Wu J Z, Zhang L J, Chen G, Wang L R, Zhao Y T, Xiao L T and Jia S T 2012 *Appl. Phys. Lett.* **101** 131114
[26] Kim J, Moal S, Portier M, Dugué J, Leduc M and Cohen-Tannoudji C 2005 *Europhys. Lett.* **72** 548
[27] Fedichev P O, Kagan Y, Shlyapnikov G V and Walraven J T M 1996 *Phys. Rev. Lett.* **77** 2913
[28] Junker M, Dries D, Welford C, Hitchcock J, Chen Y P and Hulet R G 2008 *Phys. Rev. Lett.* **101** 060406
[29] Kraemer T, Herbig J, Mark M, Weber T, Chin C, Nägerl H C and Grimm R 2004 *Appl. Phys. B* **79** 1013
[30] Li Y, Feng G, Xu R, Wang X, Wu J, Chen G, Dai X, Ma J, Xiao L and Jia S 2015 *Phys. Rev. A* **91** 053604
[31] Pichler M, Chen H and Stwalley W C 2004 *J. Chem. Phys.* **121** 1796
[32] Gerton J M, Frew B J and Hulet R G 2001 *Phys. Rev. A* **64** 053410
[33] Lange A D, Pilch K, Prantner A, Ferlaino F, Engeser B, Nägerl H C, Grimm R and Chin C 2009 *Phys. Rev. A* **79** 013622
[34] Feng G S, Li Y Q, Wang X F, Wu J Z, Sovkov V B, Ma J, Xiao L T and Jia S T 2017 *Sci. Rep.* **7** 13677
[35] Gribakin G F and Flambaum V V 1993 *Phys. Rev. A* **48** 546
[36] Chin C, Grimm R, Julienne P and Tiesinga E 2010 *Rev. Mod. Phys.* **82** 1225
[37] Chin C, Vuletić V, Kerman A J, Chu S, Tiesinga E, Leo P J and Williams C J 2004 *Phys. Rev. A* **70** 032701
[38] Kraemer T, Mark M, Waldburger P, Danzl J G, Chin C, Engeser B, Lange A D, Pilch K, Jaakkola A, Nägerl H C and Grimm R 2006 *Nature* **440** 315